

# Exact solutions for steady reconnective annihilation revisited

Vyacheslav S. Titov\*, Emanuele Tassi and Gunnar Hornig

*Theoretische Physik IV, Ruhr-Universität Bochum, 44780 Bochum, Germany*

## Abstract

This work complements the previous studies on steady reconnective magnetic annihilation in three different geometries: the two-dimensional Cartesian and polar ones and the three-dimensional (3D) cylindrical one. A special class of diffusive solutions is found analytically in explicit form for all of the three geometries. In the 3D case it is extended to a much wider class of exact solutions describing reconnective magnetic annihilation at the separatrix spine line of a magnetic null point. One of the obtained solutions provides an explicit expression for the Craig-Fabring solution. It is also identified which of the steady flow regimes found are dynamically accessible.

PACS numbers: 47.65.+a, 52.30, 96.60.R

---

\* [st@tp4.ruhr-uni-bochum.de](mailto:st@tp4.ruhr-uni-bochum.de)

## I. INTRODUCTION

Magnetic reconnection plays a key role in many phenomena of highly conducting laboratory<sup>1</sup> and space<sup>2</sup> plasmas. It provides an effective mechanism for restructuring the magnetic field and converting its energy into other forms, in particular, in solar flares and magnetospheric substorms. Therefore, magnetic reconnection is in the focus of interest for more than five decades starting from the pioneering works<sup>3,4,5,6</sup>, where its basic physics was clarified.

The highly nonlinear nature of reconnection makes it both very valuable and difficult to investigate this process in terms of exact solutions of the magnetohydrodynamic (MHD) equations, even in the simplest incompressible case. Over the last decade there has been exciting progress in this direction: many exact solutions describing a simplified form of reconnection at magnetic null points have been found in both two-dimensional<sup>7,8,9,10,11</sup> (2D) and three-dimensional<sup>12,13,14</sup> (3D) geometries. This type of reconnection will further be called magnetic reconnection annihilation following<sup>8</sup>.

The purpose of this paper is to complement previous studies by deriving the explicit form of exact solutions and their properties which had not been noticed earlier. In Sec. II we compare the existing exact solutions to identify gaps in our knowledge on them. These gaps are filled in the next sections where a class of 2D and 3D diffusive solutions is determined (Sec. III) and then extended (Sec. IV) to a wider class of 3D reconnection solutions. In Sec. IV C we analyze which of the found 3D steady solutions are accessible through a dynamic evolution. The obtained results are summarized in Sec. V.

## II. FORMULATION OF THE PROBLEM

We consider steady incompressible flows of an electrically conducting medium with uniform density  $\rho$  and resistivity  $\bar{\eta}$ . In dimensionless form they are described by the following system of MHD equations:

$$(\mathbf{v} \cdot \nabla)\mathbf{v} = -\nabla p + (\nabla \times \mathbf{B}) \times \mathbf{B}, \quad (1)$$

$$\nabla \cdot \mathbf{v} = 0, \quad (2)$$

$$\mathbf{E} + \mathbf{v} \times \mathbf{B} = \eta \nabla \times \mathbf{B}, \quad (3)$$

$$\nabla \cdot \mathbf{B} = 0, \quad (4)$$

which consists of equation of motion (1), Ohm's law (3) and divergence-free conditions (2) and (4). Here the magnetic field  $\mathbf{B}$  is normalized to its characteristic value  $B_e$ , the velocity  $\mathbf{v}$  to the Alfvén speed  $v_{Ae} \equiv B_e/\sqrt{\mu_0\rho}$  and the pressure  $p$  to twice the magnetic pressure  $B_e^2/\mu_0$ . Because of the steadiness of the flow the electric field is potential, so that by introducing the electric potential  $\Phi$  we may write

$$\mathbf{E} = -\nabla\Phi. \quad (5)$$

Let  $\mathbf{E}$  be normalized to  $v_{Ae}B_e$ , then the only dimensionless parameter in the system is the inverse magnetic Reynolds number  $\eta = \bar{\eta}/(\mu_0v_{Ae}B_e)$ .

Because of the inherent symmetry of Eqs. (1)–(5), they admit a wide variety of exact analytical solutions. In 2D case the electric field becomes simply

$$\mathbf{E} = E\hat{\mathbf{z}}, \quad E = \text{const}, \quad (6)$$

and in accordance with (2) and (4)  $\mathbf{v}$  and  $\mathbf{B}$  are expressed in terms of the stream and flux functions  $\psi(x, y)$  and  $A(x, y)$  as

$$\mathbf{v} = \nabla\psi \times \hat{\mathbf{z}}, \quad (7)$$

$$\mathbf{B} = \nabla A \times \hat{\mathbf{z}}. \quad (8)$$

Then the following ansatz in Cartesian coordinates  $(x, y)$

$$\psi(x, y) = \psi_1(x)y + \psi_0(x), \quad (9)$$

$$A(x, y) = A_1(x)y + A_0(x), \quad (10)$$

is compatible<sup>8</sup> with Eqs. (1)–(6) to yield a system of four ordinary differential equations (ODEs) for the four unknowns  $A_0(x)$ ,  $A_1(x)$ ,  $\psi_0(x)$  and  $\psi_1(x)$ . Moreover, the same ansatz but in polar coordinates, namely,

$$\psi(r, \phi) = \psi_1(r)\phi + \psi_0(r), \quad (11)$$

$$A(r, \phi) = A_1(r)\phi + A_0(r), \quad (12)$$

is also compatible<sup>9,10</sup> and it determines a curvilinear analog of the above structure in Cartesian coordinates.

In three dimensions, Eq. (6) is no longer valid in general and Eq. (5) should be used instead. Nevertheless, even in this more general case there are solutions analogous to the

ones mentioned above<sup>14</sup>. They can be written in cylindrical coordinates  $(R, \phi, z)$  by using the stream function  $\psi = R\Psi$  and flux function  $a = RA$  as follows

$$\mathbf{v} = -\nabla \times (\Psi \hat{\phi}), \quad (13)$$

$$\mathbf{B} = -\nabla \times (A \hat{\phi}), \quad (14)$$

where

$$\Psi(R, \phi, z) = \Psi_1(R)z + \Psi_0(R)\sin\phi, \quad (15)$$

$$A(R, \phi, z) = A_1(R)z + A_0(R)\sin\phi. \quad (16)$$

The corresponding streamlines and fieldlines lie in the planes  $\phi = \text{const}$  and form a structure similar (accept as  $\phi = 0$ ) to the one defined by 2D ansatz (9) and (10), as if  $x$  and  $y$  were simply changed on  $R$  and  $z$ .

The simplest solution in the case of 2D Cartesian geometry is determined by<sup>7</sup>

$$\psi = \alpha xy + A_0(x)/\alpha, \quad (17)$$

$$A = xy + A_0(x), \quad (18)$$

$$A_0 = -E \frac{2\alpha}{(1-\alpha^2)} \int_0^{x\left(\frac{1-\alpha^2}{2\alpha\eta}\right)^{1/2}} \text{daw}(X) dX, \quad (19)$$

where

$$\text{daw}(X) = e^{-X^2} \int_0^X e^{t^2} dt$$

is the Dawson integral. This solution describes the magnetic X-point configuration with an asymmetric stagnation-point flow. It is skewed along one of the two magnetic separatrices ( $x = 0$ ) by a pronounced shearing component of the flow. The flow generates a strong current layer near this separatrix by locally enhancing the role of resistivity, which makes it possible for magnetic fieldlines to cross the second separatrix when flipping from one topologically different flux region to another.

One can see that Eq. (19) has an indetermination at  $|\alpha| = 1$ , which is resolved, however, by taking into account that  $\text{daw}(X) \approx X$  at  $X \ll 1$ . Thus, Eq. (19) at  $|\alpha| \rightarrow 1$  tends to  $A_0 = -Ex^2/(2\eta)$  which gives a particular diffusive solution with the current density  $j = E/\eta$  that is uniformly distributed over the whole plane rather than concentrated near the separatrix  $x = 0$ .

The use of ansatz (9), (10) provides a two-fold generalization of Eqs. (17)–(19) characterized by two additional parameters<sup>8</sup>. However, only at a fixed value of one of them ( $\gamma = 1$  in<sup>8</sup>) this generalization admits an explicit expression. Thus, only in this case the above diffusive solution can be obtained by passing to the limit  $|\alpha| \rightarrow 1$ , while in other cases such a method does not work. A similar situation exists for the configurations described by Eqs. (11), (12) and (15), (16). In fact, in the 3D case the situation is even worse, because up to now no explicit expressions for this type of solutions were known. It is a purpose of the present paper to fill these gaps in our knowledge of the exact MHD solutions.

A comparison of Eqs. (9), (10) and (17), (18) suggests that the diffusive solutions can actually be found by imposing the additional constraint

$$\psi_1 \text{ (or } \Psi_1) = \pm A_1 \quad (20)$$

in the above 2D (or 3D) forms for exact solutions to make the respective system of ODEs slightly overdetermined. Then the diffusive solutions are derived in all three cases similarly, so only the simplest case of Eqs. (9) and (10) will be described in detail, while the rest will be given without derivation.

Before doing this, it is worth noting another important fact that has been overlooked in previous relevant studies. As it will be seen further, in the 3D solutions under consideration  $A_1 \sim R$ , which implies that the current density corresponding to Eq. (16) does not depend on  $z$  and has only two non-vanishing components

$$j_R = -\frac{(RA_0)'}{R^2} \cos \phi, \quad j_\phi = \left( \frac{(RA_0)'}{R} \right)' \sin \phi. \quad (21)$$

From here, one can then derive that

$$\mathbf{j} = \nabla \mathcal{J} \times \hat{\mathbf{z}}, \quad \mathcal{J} = -\frac{(RA_0)'}{R} \sin \phi, \quad (22)$$

where  $\mathcal{J}$  is a current function, whose iso-contours determine current lines. The vorticity in this case is similarly determined as

$$\boldsymbol{\omega} = \nabla \Omega \times \hat{\mathbf{z}}, \quad \Omega = -\frac{(R\Psi_0)'}{R} \sin \phi, \quad (23)$$

so that the iso-contours of  $\Omega$  define the vorticity lines.

### III. DIFFUSIVE SOLUTIONS

#### A. 2D Cartesian geometry

The substitution of Eqs. (6)–(10) into Eqs. (1)–(4) yields a system of four ODEs (see<sup>8</sup>). With the help of Eq. (20) one of them is satisfied by the requirement  $|\alpha| = 1$ , while the others are reduced after simple transformations to

$$A_1'' = 0, \quad (24)$$

$$A_1(\psi_0 \mp A_0)'' - A_1'(\psi_0 \mp A_0)' = \pm q, \quad (25)$$

$$E + A_1(\psi_0 \mp A_0)' + \eta A_1'' = 0, \quad (26)$$

where  $q$  is an arbitrary constant and the dash denotes the derivative with respect to  $x$ . The structure of the equations suggests an obvious way to solve them: first, find  $A_1$  from Eq. (24) and substitute it into Eqs. (25) and (26); secondly, find the combination  $\psi_0 \mp A_0$  from Eq. (25) and substitute it into Eq. (26) to obtain  $A_0$ . This results in

$$A_1 = hx + C_0, \quad (27)$$

$$\psi_0 \mp A_0 = C_1 \frac{x^2}{2} \mp \frac{q}{h}x + C_2, \quad (28)$$

$$A_0 = \frac{1}{\eta} \left( -C_1 h \frac{x^4}{12} \pm q \frac{x^3}{6} - E \frac{x^2}{2} \right) + C_3 x + C_4, \quad (29)$$

where the gradient of magnetic field  $h$  and other constants of integration  $C_i$ ,  $i = 0, \dots, 4$ , are arbitrary. One can always choose  $C_0 = C_3 = 0$  by bringing the origin of the coordinate system to the magnetic null point of the configuration under study. For this point we are also free to fix  $\psi(0, 0) = A(0, 0) = 0$ , which means that  $C_2 = C_4 = 0$ .

The remaining constants  $C_1$ ,  $E$  and  $q$  are expressed in terms of the physical parameters at  $\mathbf{r} = \mathbf{0}$  such as vorticity  $\omega_0 \equiv -\nabla^2 \psi(0, 0)$ , current density  $j_0 \equiv -\nabla^2 A(0, 0)$  and velocity  $v_{y0} \equiv v_y(0, 0)$  to give  $C_1 = \pm j_0 - \omega_0$ ,  $E = \eta j_0$  and  $q = \pm h v_{y0}$ . It is reasonable also to require that in the ideal MHD limit  $\eta \rightarrow 0$  the value  $A_0$  remains finite. This is achieved by introducing instead of  $\omega_0$  and  $v_{y0}$  the new parameters  $w$  and  $u$  such that

$$\omega_0 = \pm j_0 + \eta w, \quad (30)$$

$$v_{y0} = \eta u. \quad (31)$$

Thus, the above consideration yields

$$\psi = \pm A - \eta \left( w \frac{x^2}{2} + ux \right), \quad (32)$$

$$A = h \left( w \frac{x^4}{12} + u \frac{x^3}{6} \right) - j_0 \frac{x^2}{2} + hxy. \quad (33)$$

Here the first term in  $\psi$  describes the flow component aligned with the magnetic fieldlines, while the second term corresponds to a shearing flow parallel to the  $y$ -axis and so transversal to the fieldlines.

This shearing flow is due to a plasma diffusion caused by resistive dissipation of a non-potential part of the magnetic field (first term in Eq. (33)), which is created by the non-uniform current density

$$j = j_0 - h(wx^2 + ux). \quad (34)$$

The resistive diffusion provides also a shift of the stagnation point of the flow with respect to the magnetic null point along  $y$ -axis, so that its coordinate grows linearly with  $\eta$  as follows

$$y_0 = \pm \eta u / h. \quad (35)$$

The same effect is responsible for the presence of the resistive uniform addition to the vorticity

$$\omega = \pm j + \eta w. \quad (36)$$

Compared to the diffusive solution obtained as a limiting case  $\alpha = 1$  of the Craig-Henton solution, this new class of solutions is characterized by two additional dimensionless parameters  $w$  and  $u$  to give more inhomogeneous and non-symmetric structures of the magnetic field and flow which are sustained by a one-dimensional parabolic distribution of the current density. An illustrative example of the magnetic fieldlines and streamlines superimposed onto the current density distribution of this solution is shown in Fig. 1(a).

The pressure in the considered case is given by

$$p = p_0 + qy - \frac{1}{2}(B_x^2 + B_y^2), \quad (37)$$

where  $B_x = hx$  and  $B_y = -(A'_0 + hy)$ . This expression shows that the pressure is positive in a finite region around the null point if the constant  $p_0$  characterizing the pressure at this point is large enough, therefore only such values of  $p_0$  are physically admissible.

## B. 2D curvilinear geometry

Assume that the polar coordinates  $(r, \phi)$  are related to the Cartesian ones  $(x, y)$  as

$$x = r \sin \phi, \quad y = r \cos \phi - d. \quad (38)$$

Choosing here only positive values for the parameter  $d$ , we place the pole  $r = 0$  below the line  $y = 0$  or, in other words, out of the half-plane  $y \geq 0$ , where the curvilinear analog of the above solutions will be considered. Using Eqs. (6)–(8), (11) and (12) one can derive from Eqs. (1)–(4) a system of four ODEs, which after imposing additional constraint (20) can be integrated to yield

$$\psi = \pm A - \eta \left[ \frac{w}{4}(r^2 - r_0^2) + r_0 \left( w \frac{r_0}{2} - u \right) \ln \left( \frac{r_0}{r} \right) \right], \quad (39)$$

$$A = \frac{1}{8}(hw - 2j_0)(r^2 - r_0^2) + \frac{1}{8} [hw(r^2 + r_0^2) - 4j_0r_0^2] \ln \left( \frac{r_0}{r} \right) - \frac{h}{12}r_0(wr_0 - 2u) \ln \left( \frac{r_0}{r} \right)^3 + h\phi \ln \left( \frac{r_0}{r} \right). \quad (40)$$

Here the radius at which both  $A_1$  and  $\psi_1$  vanish is denoted by  $r_0$ , while the other notations are chosen by analogy with the previous case, namely,  $\omega_0 \equiv -\nabla^2\psi(r_0, 0)$ ,  $j_0 \equiv -\nabla^2 A(r_0, 0)$ ,  $v_{\phi 0} \equiv v_\phi(r_0, 0)$ ,  $w = (\omega_0 \mp j_0)/\eta$  and  $u = v_{\phi 0}/\eta$ . Although this solution is obviously multi-valued, we may always choose only one of its branches by restricting its domain of definition, say, to the half-plane  $y \geq 0$ , which makes such a solution physically meaningful.

In spite of a significant difference in the form of solutions obtained in polar and Cartesian coordinates, the corresponding structures of MHD flows in both cases are quite similar (see Fig. 1). Indeed, Eqs. (39) and (40) define an asymmetrical neighborhood of a magnetic null point located at  $(r = r_0, \phi = 0)$  with the flow that consists of a strong field-aligned component and a slight shearing azimuthal component caused by resistive diffusion of plasma across magnetic fieldlines. Owing to this diffusion the corresponding stagnation point is shifted to the angle  $\phi = \mp \eta u r_0 / h$  along the arc  $r = r_0$ , which is a separatrix line for both the velocity and magnetic fields. The current density distribution depends only on radius  $r$  in the form

$$j = j_0 - \frac{h}{r^2} \ln \left( \frac{r_0}{r} \right) \left[ \frac{w}{2}(r^2 - r_0^2) + u r_0 \right], \quad (41)$$

where the non-uniform part is proportional to the parameters  $u$  and  $w$ . They enter similarly into the resistive term of Eq. (39), therefore the plasma diffusion in the considered flow is closely related to the inhomogeneity of the resistive dissipation of the current.

The expression for the pressure

$$p = p_0 - \int \frac{B_\phi^2 - v_\phi^2}{r} dr - \frac{1}{2}(B_r^2 + B_\phi^2) \quad (42)$$

is more complicated in this case than before, but it reduces to Eq. (37) in the limit of vanishing curvature. Other physical values in the same limit also reduce to the required expressions.

### C. 3D cylindrical geometry

Substituting Eqs. (13) and (14) into Eqs. (1)–(4) under the assumption that  $\Psi$  and  $A$  are defined by Eqs. (15) and (20), one can obtain a system of ODEs whose regular solution is

$$\Psi = \pm A + \frac{1}{4}\eta\lambda R^3 \sin \phi, \quad (43)$$

$$A = hRz - \left( j_0 + \frac{2h\lambda}{15} R^3 \right) \frac{R^2}{3} \sin \phi, \quad (44)$$

where

$$h \equiv \left. \frac{\partial B_R}{\partial R} \right|_{\mathbf{r}=\mathbf{0}}, \quad (45)$$

$$j_0 \equiv (\nabla \times \mathbf{B})_x \Big|_{\mathbf{r}=\mathbf{0}}, \quad (46)$$

$$\lambda \equiv -\frac{1}{3\eta} (\nabla^2 \mathbf{v})_z \Big|_{(R=0, \phi=\pi/2)}. \quad (47)$$

The 3D velocity and magnetic fields described by this solution both contain null points that coincide with each other and are located at the origin of the coordinate system ( $\mathbf{r} = \mathbf{0}$ ).

In the limit of vanishing resistivity ( $\eta \rightarrow 0$ ), the corresponding configuration becomes simply a field-aligned flow whose potential and non-potential components are represented, respectively, by the first and second terms in Eq. (44). The potential component  $hRz$  corresponds to a null point configuration that is cylindrically symmetric about  $z$ -axis. The non-potential component is a shearing motion parallel to the  $z$ -axis and such that its vorticity

and current density are given by

$$\pm\omega_R = j_R = \left( j_0 + \frac{4}{15}\lambda h R^3 \right) \cos \phi, \quad (48)$$

$$\pm\omega_\phi = j_\phi = - \left( j_0 + \frac{16}{15}\lambda h R^3 \right) \sin \phi, \quad (49)$$

so that the corresponding current function  $\mathcal{J}$  [see Eq. (22)] has the following form:

$$\mathcal{J} = -R \left( j_0 + \frac{4}{15}\lambda h R^3 \right) \sin \phi. \quad (50)$$

The iso-contours of  $\mathcal{J}$  representing the current fieldlines are shown in Fig. 2. In the resistive case, the vorticity takes on an additional term to become

$$\omega_R = \pm j_R - \eta\lambda R \cos \phi, \quad \omega_\phi = \pm j_\phi + 2\eta\lambda R \sin \phi, \quad (51)$$

so that the corresponding vorticity function is

$$\Omega = \pm\mathcal{J} + \eta\lambda R^2 \sin \phi. \quad (52)$$

It shows that the resistivity leads to a certain deviation of the vorticity lines from the current lines. They deviate towards (outwards) the null point (Fig. 2) if the vorticity is counter-directed (co-directed) to the current density.

This is a result of the resistive diffusion of plasma elements across magnetic fieldlines, which can directly be seen from Eqs. (43) and (44). Indeed, as follows from Sec. II, the streamlines and fieldlines in our case lie at the intersections of the planes of constant  $\phi$  with the surfaces  $R\Psi = \text{const}$  and  $RA = \text{const}$ , respectively. According to Eq. (43), however, the resistive addition in  $\Psi$  has a different dependence on  $R$  than  $A$ , therefore the streamlines must cross fieldlines at some points [Fig. 3(a)], which just means the above mentioned diffusion.

The magnetic flux surfaces shown in Figure 3(b) demonstrate that the whole configuration can be interpreted as a neighborhood of an axisymmetric magnetic null point skewed along the  $z$ -axis by a shearing deformation. The steady structure is sustained by a stagnation flow whose streamlines are similar to the fieldlines – exactly as it was in the analogous 2D flows considered above. But, contrary to them, a shift of the stagnation point with respect to the magnetic null point is not present in our diffusive 3D flow. This, however, does not mean that such a shift is not possible in the 3D case, rather it points out that ansatz (15), (16) is not a full analogy to Eqs. (9), (10).

This can also be seen from comparison of the corresponding expressions for the pressure, which in our 3D case is

$$p = p_0 - \frac{1}{2}(v_R^2 + B_z^2). \quad (53)$$

Here also  $v_R = B_R$  and so  $p + B^2/2 = p_0$ , which, in turn, implies that the plasma acceleration  $(\mathbf{v} \cdot \nabla)\mathbf{v}$  in this case is caused exclusively by the magnetic tension  $(\mathbf{B} \cdot \nabla)\mathbf{B}$ . Contrary to this, in the 2D case the pressure gradient  $q$  along the  $y$ -axis does contribute to the plasma acceleration.

#### IV. EXPLICIT SOLUTIONS FOR SPINE RECONNECTIVE ANNIHILATION

##### A. Derivation of solutions

Consider now the subclass of exact solutions which satisfy Eqs. (15) and (16) but not necessarily Eq. (20). After passing to the new independent variable  $s = R^2/2$  and unknowns  $a_0 = RA_0$ ,  $a_1 = RA_1$ ,  $\psi_0 = R\Psi_0$ ,  $\psi_1 = R\Psi_1$ , the substitution of Eqs. (15) and (16) into Eqs. (1)–(4) yields<sup>14</sup> the following system of ODEs:

$$a_1\psi_1' - \psi_1a_1' + 2\eta s a_1'' = 0, \quad (54)$$

$$\psi_1\psi_1'' - \psi_1'^2 - a_1a_1'' + a_1'^2 = -k, \quad (55)$$

$$(a_1\psi_0' - \psi_1a_0' + 2\eta s a_0'')' = \frac{\eta}{2s}a_0', \quad (56)$$

$$\psi_1\psi_0'' - \psi_1'\psi_0' - a_1a_0'' + a_1'a_0' = 0, \quad (57)$$

where  $k$  is an arbitrary constant. Mellor et al.<sup>14</sup> solved these equations approximately by using the method of matched asymptotic expansions in small parameter  $\eta$ . In particular, they noticed that the values

$$a_1 = 2B_{Re}s, \quad \psi_1 = 2v_{Re}s, \quad (58)$$

may serve as an outer solution of Eqs. (54) and (55) provided that

$$k = 4(v_{Re}^2 - B_{Re}^2), \quad (59)$$

where the constants  $B_{Re}$  and  $v_{Re}$  are  $R$ -components of  $\mathbf{B}$  and  $\mathbf{v}$  at  $R = 1$ . A straightforward proof, however, shows that this solution is actually exact rather than approximate. The latter makes it possible to solve the rest of the system of equations explicitly.

Indeed, after introducing the new unknown

$$F_0 = v_{Re}\psi'_0 - B_{Re}a'_0, \quad (60)$$

Eq. (57) reduces to

$${}_sF'_0 - F_0 = 0, \quad (61)$$

which is immediately integrated to give

$$F_0 = C_1 s. \quad (62)$$

Using Eqs. (60) and (62) to eliminate  $\psi'_0$  in Eq. (56) and changing the independent variable  $s$  to

$$S = \frac{|\kappa|}{\eta} s \equiv \frac{|\kappa|}{2\eta} R^2, \quad \kappa = \frac{v_{Re}^2 - B_{Re}^2}{2v_{Re}}, \quad (63)$$

we obtain

$$S^2 a_0''' - S(\pm 2S - 1)a_0'' - \left(\pm 2S + \frac{1}{4}\right) a_0' \pm \tilde{C}_1 S^2 = 0, \quad (64)$$

where

$$\tilde{C}_1 = \frac{2\eta^2 B_{Re}}{\kappa^3 v_{Re}} C_1 \quad (65)$$

and the upper plus (lower minus) corresponds to positive (negative) sign of  $\kappa$ . It is remarkable that the obtained equation admits a general solution in explicit form such that (see Appendix for details)

$$a'_0(S) = \tilde{C}_1 F_{1\pm}(S) + C_2 F_{2\pm}(S) + C_3 F_{3\pm}(S), \quad (66)$$

$$F_{1\pm}(S) = F_{2\pm}(S) \int_{\infty}^S e^{\mp\tau} \tau^{3/2} (K_0(\tau) \mp K_1(\tau)) d\tau \\ - F_{3\pm}(S) \int_0^S e^{\mp\tau} \tau^{3/2} (I_0(\tau) \pm I_1(\tau)) d\tau, \quad (67)$$

$$F_{2\pm}(S) = e^{\pm S} \sqrt{S} (I_0(S) \pm I_1(S)), \quad (68)$$

$$F_{3\pm}(S) = e^{\pm S} \sqrt{S} (K_0(S) \mp K_1(S)), \quad (69)$$

where  $I_i$  and  $K_i$ ,  $i = 0, 1$ , are modified Bessel functions of zero and first orders of the respective arguments. The lower limits in the integrals of Eq. (67) may be chosen arbitrary,

because this leads only to a redefinition of the constants of integration  $C_2$  and  $C_3$ . We used this freedom to minimize asymptotic growth of  $F_{1+}(S)$  by choosing  $\infty$  for the lower limit in the first integral of Eq. (67), instead of 0 in other cases.

Taking into account Eqs. (60), (62) and (63), we obtain

$$\psi'_0(S) = \frac{B_{Re}}{v_{Re}} a'_0(S) + \frac{\eta}{|\kappa|v_{Re}} C_1 S, \quad (70)$$

which determines together with Eqs. (66)–(69) and (58) a subclass of exact solutions of Eqs.(54)–(57) in explicit form.

## B. Basic properties of solutions

To interpret the solution found, note first that its velocity and magnetic field are naturally decomposed as

$$\mathbf{v} = \mathbf{v}_1 + \mathbf{v}_0, \quad \mathbf{B} = \mathbf{B}_1 + \mathbf{B}_0, \quad (71)$$

where the components 1 and 0 correspond to the parts of  $\psi$  and  $A$  marked by the same indices. From Eqs. (13), (14) and (58) it follows that they have the form:

$$\mathbf{v}_1 = v_{Re}(R\hat{\mathbf{R}} - 2z\hat{\mathbf{z}}), \quad \mathbf{v}_0 = -\frac{|\kappa|}{\eta} \psi'_0(S) \sin \phi \hat{\mathbf{z}}, \quad (72)$$

$$\mathbf{B}_1 = B_{Re}(R\hat{\mathbf{R}} - 2z\hat{\mathbf{z}}), \quad \mathbf{B}_0 = -\frac{|\kappa|}{\eta} a'_0(S) \sin \phi \hat{\mathbf{z}}. \quad (73)$$

Both components here represent field-aligned flows of two different types: the component 1 is a flow along the fieldlines of an axisymmetric null point such that its separatrix spine line coincides with the  $z$ -axis, while the component 0 is a shearing flow parallel to the spine. The superposition of these two components results again in a field-aligned flow only if

$$\frac{\psi'_0(S)}{a'_0(S)} = \frac{v_{Re}}{B_{Re}}, \quad (74)$$

otherwise, the resulting flow has always a transverse component. We will call such a flow reconnective if the transverse component does not vanish at the separatrix fan surface when  $\eta \rightarrow 0$ . However, if the transverse motion vanishes in this limit, the flow will be called diffusive. The diffusive solutions considered in Sec. III C provide an example of such flows.

Since the component 0 is a linear superposition of three independent solutions, it has been studied by analyzing each of them separately. Table I summarizes their asymptotic

behavior at small and large  $S$  and classifies these solutions on diffusive and reconnective according to the above definition.

Figure 4 shows that  $F_{1\pm}$  noticeably deviates from a linear dependence on  $S$  only at  $S \lesssim 0.3 \mp 0.2$ , which corresponds to  $R \lesssim (0.7 \mp 0.3)\sqrt{\eta/|\kappa|}$ . Direct calculations demonstrate that everywhere outside this region Eq. (74) is fulfilled for  $F_{1\pm}$  in the limit of vanishing  $\eta$ . This means that the respective flows are nearly field-aligned or, in other words, diffusive. The current lines, magnetic fieldlines and flux surfaces corresponding to this solution are quite similar to those we had for the solutions in Sec. III C (see Fig. 2 and 3). So it describes, as before, the neighborhood of an axisymmetric null point skewed by a shearing deformation along the  $z$ -axis.

Analyzing the solution based on  $F_{2+}(S)$ , we assume for the definiteness that the volume where this solution is applicable is restricted in radial direction by radii  $R \leq 1$ . Note also that the function  $F_{2+}(S)$  grows exponentially with  $S$ , so to keep the boundary values  $B_{0z}|_{R=1}$  and  $v_{0z}|_{R=1}$  finite at vanishing  $\eta$ , it is necessary to require that  $C_{2+} \sim \eta e^{-|\kappa|/\eta}$ . Such a requirement makes the respective solution physically admissible, but at the cost of having  $v_{0z}$  and  $B_{0z}$  to exponentially decay towards  $R = 0$ . Thus, all the variation of physical values occurs in a thin boundary layer at  $R = 1$  such that  $\mathbf{v}_0$  and  $\mathbf{B}_0$ , and hence the transverse motion, are negligible in the volume at small  $\eta$ . Therefore this solution is also diffusive, although Eq. (74) is not fulfilled in this case.

The solution based on  $F_{2-}(S)$  is actually an explicit representation of the previous Craig-Fabring solution<sup>13</sup>, whose properties become more evident in this new representation. For this solution  $F_0(S) = 0$  and, hence, [see Eq. (60)] instead of Eq. (74) the reverse ratio is valid. By comparing also Eqs. (72) and (73) with the asymptotics of  $F_{2-}(S)$  we see that  $v_{0z}$  and  $B_{0z}$  remain finite far from the spine, which means that this solution is indeed reconnective, as shown first in<sup>13</sup>. The magnetic reconnection here is caused by the resistive dissipation of the current concentrated in two adjacent rolls parallel to the spine line. The current concentration is sustained, first, by the shearing  $\mathbf{v}_0$ -flow that stretches the fieldlines along the spine and, second, by the  $\mathbf{v}_1$ -flow that folds them up towards the spine when  $v_{Re} < 0$  (see Fig. 5). The characteristic size of the dissipative current rolls is determined from  $S \simeq 0.34$  at which  $F_{2-}(S)$  attains its maximum [see Fig. 4(b)], therefore this size scales as  $\sim \sqrt{\eta/|\kappa|}$ .

The remaining solutions based on  $F_{3\pm}(S)$  seem to be not admissible, since they both

have a singularity at  $R = 0$ . Nevertheless, it is worth discussing their properties as well, because the singularities may sometimes appear even in dissipative processes. This occurs dynamically in the so-called blow-up regimes<sup>16</sup> and, a priori, we cannot exclude the possibility of saturation of such regimes at some singular steady states similar the ones described by  $F_{3\pm}(S)$ .

The solution  $F_{3+}(S)$  is reconnective as  $F_{2-}(S)$ , because at large  $S$  they both behave similarly. At small  $S$ , however, their behavior is opposite of each other: as just mentioned,  $F_{3+}(S)$  diverges rather than vanishes at  $S = 0$ . The current lines of this solution form two parallel rolls as before, but now they are pressed towards each other to produce a kind of line-dipole singularity at the  $z$ -axis [Fig. 6(a)].

The separatrix structures defined in both cases by  $RA = 0$  are also different. In the case of the  $F_{2-}$  solution, the condition  $RA = 0$  defines a two-component structure consisting of the spine line  $R = 0$  which pierces through the fun flux surface. The shape of the latter can be imagined to be the result of bulging the flat surface  $z = 0$  up and down along the current rolls [Fig. 5(b)] proportionally to the local values of current density. The separatrix surface of the  $F_{3+}$  solution is obtained in a similar way, but now the bulging goes to its extreme at the current singularity with pulling the  $z = 0$  surface to plus or minus infinity of the  $z$ -axis depending on the roll [Fig. 6(b)]. This yields a one-component separatrix structure that is glued of two crater-like surfaces one of which is turned upside-down.

The properties of  $F_{3-}$  solution are similar, except that the whole structure is now more concentrated to the  $z$ -axis, because  $F_{3-}(S)$  decays exponentially with distance from the origin. The latter means also that such a solution is diffusive.

The dependence of the obtained solutions on the sign of the parameter  $\kappa$  has several important implications. If  $\kappa$  is negative, then either  $|v_{Re}| < |B_{Re}|$  and  $v_{Re} > 0$  or  $|v_{Re}| > |B_{Re}|$  and  $v_{Re} < 0$  [see Eq. (63)]. The first case corresponds to sub-Alfvénic  $\mathbf{v}_1$ -outflows (from the spine), while the second case corresponds to super-Alfvénic  $\mathbf{v}_1$ -inflows (to the spine). Similarly, in the case of positive  $\kappa$  there are two possibilities – either sub-Alfvénic  $\mathbf{v}_1$ -inflows or super-Alfvénic  $\mathbf{v}_1$ -outflows. The intermediate case of  $\kappa = 0$  corresponds to the diffusive solutions with Alfvénic  $\mathbf{v}_1$ -flows which have already been considered in Sec. III C. Here we just point out that they can be recovered from regular branches of Eqs. (66)–(70) as leading terms of the respective Taylor expansions at  $S = 0$ .

### C. Dynamically accessible steady flows

In connection with the obtained solutions an important question arises: which of them are physically feasible? This question concerns not only the singular solutions, but also the different branches of regular solutions depending on the sign of  $\kappa$  and direction of the  $\mathbf{v}_1$ -flow. There is no way to resolve this question or even to make it more precise, remaining in the framework of the steady state formulation of the problem. This can be done only by considering the transitional process in which the system is driven by a suitable variation of boundary conditions from the initial  $\mathbf{B}_1$ -field with the  $\mathbf{v}_1$ -flow to one of the above steady states. To remain in the scope of the present work, we present here only a summary of such a consideration, while the full study will be published elsewhere.

Assuming that the velocity and magnetic field are decomposed as before [see Eqs. (71)–(73)] except that  $\mathbf{v}_0$  and  $\mathbf{B}_0$  now depend additionally on time  $t$  and initially equal zero, it is possible to derive a compatible system of two linear partial differential equations for two unknowns  $a'_0(s, t)$  and  $\psi'_0(s, t)$ . Their parts with spatial derivatives are determined simply by Eqs. (56) and (57), while the additional first order time derivatives of  $a'_0$  and  $\psi'_0$  enter, respectively, into the first and second equation.

The equations in such a system are coupled and, strictly speaking, a prescription of the boundary conditions for each of them is interrelated. However, the time-dependent analog of Eq. (56) contains the time derivative of only  $a'_0$  and its highest spatial derivatives. It can heuristically understood then as a parabolic second order equation for  $a'_0$ , where the terms with  $\psi'_0$  are source terms. “The equation for  $\psi'_0$ ” can be understood in a similar way to identify it as a hyperbolic first order equation with the characteristics based on the  $\mathbf{v}_1$ -field. Taken together, this implies that, if the problem is studied on the interval  $0 \leq R \leq 1$ ,  $a'_0$  can be imposed at both its ends, while  $\psi'_0$  only at one of them and only upstream the  $\mathbf{v}_1$ -flow.

The numerical experiments confirm this heuristic rule for possible boundary conditions. They show that the steady flows based on the  $F_{1\pm}$ -solutions are accessible during the above evolution in both outflow and inflow regimes, while the  $F_{2\pm}$ -solutions are realizable only in the inflow regime (see Table I). There was no sign of blow up of the structure at the spine in these experiments, so the steady flows based on the  $F_{3\pm}$ -solutions are not accessible dynamically from the boundary  $R = 1$  and therefore these solutions should be discarded. As seen from Table I, the reconnective flows can in general realize only through a linear combination

of the  $F_{2-}$ - and  $F_{1-}$ -solutions in the regime with the super-Alfvénic  $\mathbf{v}_1$ -inflow. Taking also into account the incompressible character of the flows, this imposes severe limitations on the conditions where such reconnective flows may occur – applying to the Sun, for example, these should be photospheric rather than coronal conditions.

## V. SUMMARY

A comparative analysis of the existing exact MHD solutions for steady reconnective magnetic annihilation in three different geometries is performed to reveal several gaps in our knowledge on such solutions. These gaps are filled in this paper by presenting the new explicit expressions for the so-called diffusive solutions and for a much wider subclass of exact solutions describing spine reconnective annihilation. In particular, we have found an explicit expression of the Craig-Fabring solution in terms of the modified Bessel functions of zero and first order. The properties of the obtained solutions for spine reconnection are considered in detail. We have also identified which of the found steady flow regimes are accessible through a dynamic evolution. This consideration confirms that the Craig-Fabring flow is a major reconnective constituent of the MHD flows described by such solutions.

### Acknowledgments

The authors gratefully acknowledge financial support from the Volkswagen-Foundation and EU grant No. HPRN-CT-2000-00153.

### APPENDIX A: SOLVING EQ. (64)

This is a second-order linear equation on  $a'_0(S)$ , so its general solution is a superposition of two homogeneous solutions and a particular inhomogeneous one. It is sufficient to find the homogeneous solutions, while the particular one can then be found by the method of variation of parameter. Note first that with the substitution  $a'_0(S) = e^{\mp S} \sqrt{S} Z(S)$  Eq. (64) reduces to the form

$$SZ'' + 2Z' - (S \pm 1)Z = 0, \tag{A1}$$

which can be derived, in turn, from the modified Bessel equation of zero order

$$Sf'' + f' - Sf = 0, \tag{A2}$$

whose solution is  $f(S) = I_0(S)$  or  $K_0(S)$ . Indeed, differentiating this equation yields

$$Sf''' + 2f'' - Sf' - f = 0, \tag{A3}$$

so that after adding or subtracting it from Eq. (A2), we obtain Eq. (A1) in which

$$Z = f \pm f'. \tag{A4}$$

Taking also into account the identities  $I_0'(S) = I_1(S)$  and  $K_0'(S) = -K_1(S)$ , one arrives at Eqs. (68) and (69), while Eq. (67) is then obtained by the method of variation of parameter.

- 
- <sup>1</sup> D. Biskamp *Magnetic reconnection in plasmas* (Cambridge Univ. Press, Cambridge, 2000).
- <sup>2</sup> E. R. Priest, and T. G. Forbes, *Magnetic reconnection* (Cambridge University Press, Cambridge, 2000).
- <sup>3</sup> J. W. Dunjey, *Philos. Mag. Ser. 7* **44**, 725 (1953).
- <sup>4</sup> E. N. Parker, *J. Geophys. Res.* **62**, 509 (1957).
- <sup>5</sup> P. A. Sweet, in *Electromagnetic Phenomena in Cosmical Physics*, IAU Symp. **6**, ed. B. Lehnert, (Cambridge Univ. Press, London, 1958) p. 123.
- <sup>6</sup> H. E. Petschek, in *Physics of solar flares*, ed. W. N. Hess (NASA SP-50, Washington, DC, 1964) p. 425.
- <sup>7</sup> I. J. D. Craig, and S. M. Henton, *Astrophys. J.* **450**, 280 (1995).
- <sup>8</sup> E. R. Priest, V. S. Titov, R. E. Grundy, and A. W. Hood, *Proc. R. Soc. Lond. A* **456**, 1821 (2000).
- <sup>9</sup> E. Tassi, V. S. Titov, and G. Hornig, *Phys. Lett. A* **302**, 313 (2002).
- <sup>10</sup> P. G. Watson, and I. J. D. Craig, *Sol. Phys.* **207**, 337 (2002).
- <sup>11</sup> E. Tassi, V. S. Titov, and G. Hornig, *Phys. Plasmas* **10**, 448 (2003).
- <sup>12</sup> I. J. D. Craig, R. B. Fabling, S. M. Henton, and G. J. Rickard, *Astrophys. J.* **455**, L197 (1995).
- <sup>13</sup> I. J. D. Craig and R. B. Fabling, *Astrophys. J.* **462**, 969 (1996).
- <sup>14</sup> C. Mellor, E. R. Priest and V. S. Titov, *Geophys. Astrophys. Fluid Dynamics* **96**, 153 (2002).
- <sup>15</sup> E. R. Priest, and V. S. Titov, *Phil. Trans. Roy. Soc. Lond. A* **354**, 2951 (1996).
- <sup>16</sup> V. A. Galaktionov, and J. L. Vazquez, *Discr. Cont. Dyn. Sys. A* **8**, 399 (2002).

<b>Limit:</b> \ $F \sim$ :	$F_{1+} \sim$	$F_{1-} \sim$	$F_{2+} \sim$	$F_{2-} \sim$	$-F_{3+} \sim$	$F_{3-} \sim$
$S \rightarrow 0$	$0.185\sqrt{S}$	$\frac{4}{15}S^2$	$\sqrt{S}$	$\sqrt{S}$	$\frac{1}{\sqrt{S}}$	$\frac{1}{\sqrt{S}}$
$S \rightarrow \infty$	$\frac{S}{4} + \frac{3}{32}$	$\frac{S}{4} - \frac{3}{32}$	$\sqrt{\frac{2}{\pi}}e^{2S}$	$\frac{1}{\sqrt{8\pi S}}$	$\sqrt{\frac{\pi}{2}}\frac{1}{S}$	$\sqrt{2\pi}e^{-2S}$
<b>Flow type:</b>	D	D	D	R	R	D
<b>Accessible as:</b>	$\text{in}^{\text{out}}\text{A}$	$\text{out}^{\text{in}}\text{A}$	$\text{inA}$	$\text{inA}$		
<b>Admissible?</b>	yes	yes	yes	yes	no	no

TABLE I: Asymptotic behavior of the independent solutions entering linearly into  $a'_0(S)$ , the type of the corresponding flows (diffusive D or reconnective R), their dynamical accessibility (e.g.,  $\text{inA}$  denotes the structure with sub-Alfvénic  $\mathbf{v}_1$ -inflows, while  $\text{out}^{\text{in}}\text{A}$  corresponds to super-Alfvénic  $\mathbf{v}_1$ -outflows) and the physical admissibility of solutions.

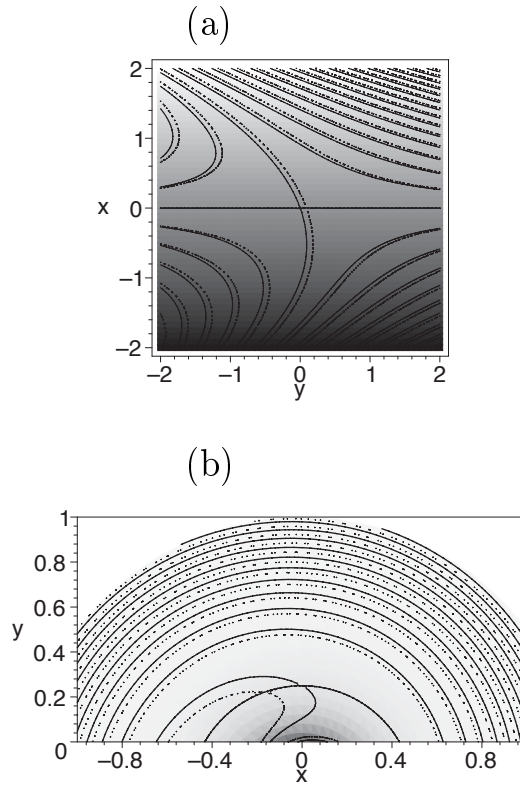


FIG. 1: Fieldlines (solid) and streamlines (dotted) superimposed onto the current density distribution shown in gray half-tones at the following parameters: (a)  $h = 15.9$ ,  $w = -0.01$ ,  $u = 2.07$ ,  $j_0 = 11.4$  and  $\eta = 0.7$  (Cartesian coords.); (b)  $d = 0.25$ ,  $r_0 = 0.5$ ,  $h = 7.3$ ,  $w = 35.0$ ,  $u = 50.4$ ,  $j_0 = 100.0$ , and  $\eta = 0.1$  (polar coords.).

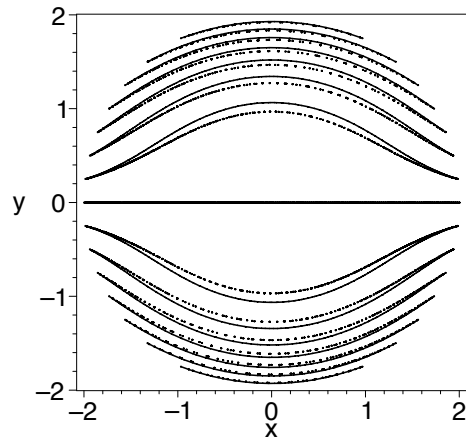


FIG. 2: Current lines (solid) at  $j_0 = 0.043 h\lambda$  and vorticity lines (dotted) at  $\lambda/h = 3.0$  and  $\eta = 0.3$  when the vorticity is counter-directed to the current density.

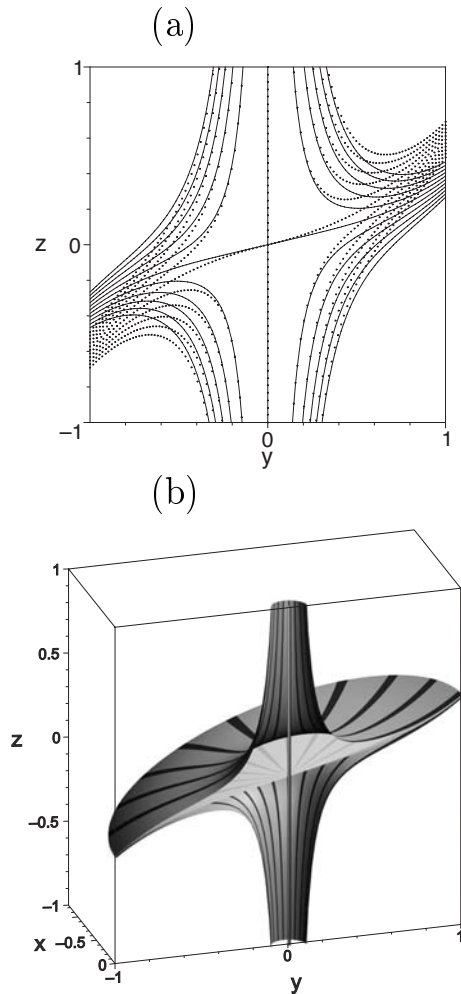


FIG. 3: (a) Fieldlines (solid) and streamlines (dotted) in the plane  $x = 0$ . (b) Three magnetic flux surfaces  $RA = 0, \pm 0.01$  cut off by the plane  $x = 0$ ; the mid surface  $RA = 0$  is a union of the separatrix fan surface and the spine line (parallel to  $z$ -axis, for more about fan surfaces and spine lines see<sup>15</sup>) with the intersection at the null point. The fieldline structure is depicted by strips shaded in dark gray. For both plots  $h = 1.0$ ,  $j_0 = 0.7$  and  $\lambda = 3.0$ .

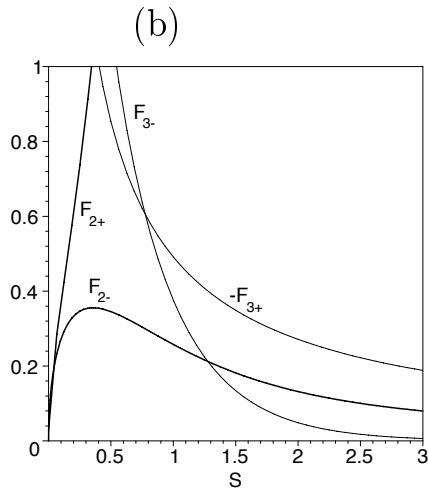
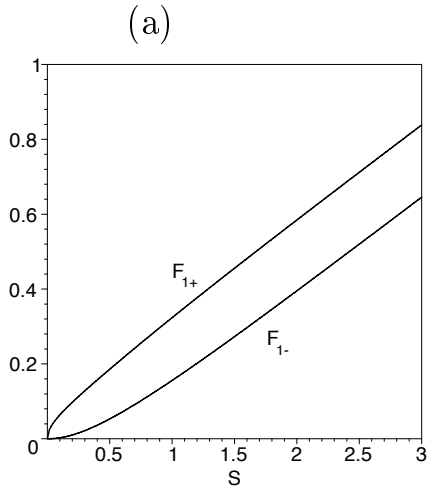


FIG. 4: (a) Inhomogeneous solutions for positive and negative  $\kappa$ . (b) Homogeneous solutions. Physically admissible solutions are shown by thick lines.

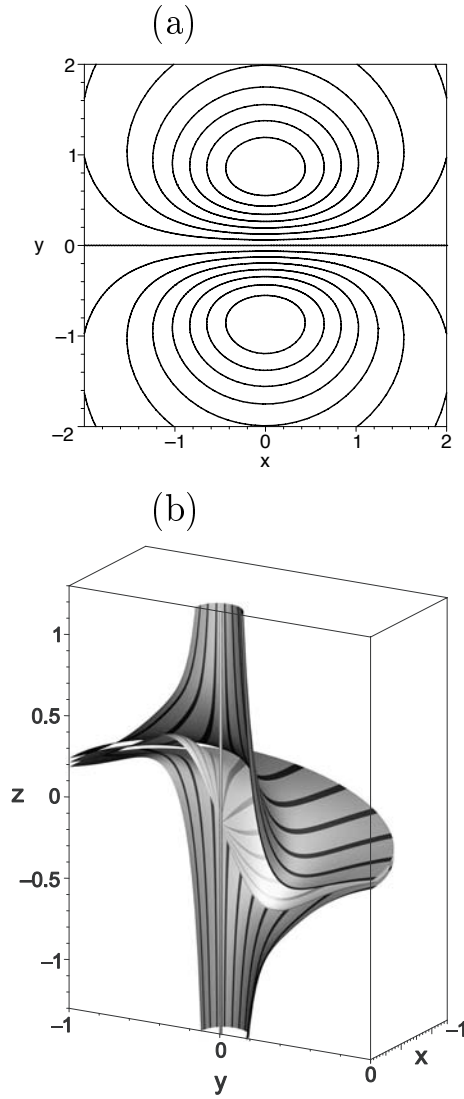


FIG. 5: (a) Current lines corresponding to  $F_{2-}$  solution (Craig-Fabring solution). (b) Three magnetic flux surfaces  $RA = 0, \pm 0.164$  cut off by the plane  $x = 0$ ; the mid surface  $RA = 0$  is a union of the separatrix fan surface and spine line (parallel to  $z$ -axis) with the intersection at the null point. The parameters are  $B_{Re} = 1$ ,  $|\kappa|/\eta = 1.83$ ,  $C_2 = 1.64$ .

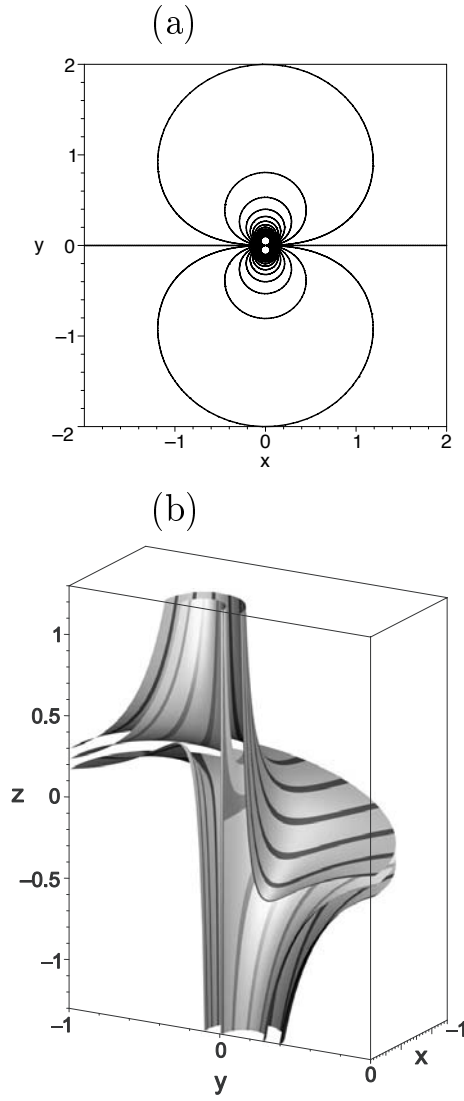


FIG. 6: (a) Current lines corresponding to  $F_{3+}$  solution. (b) Three magnetic flux surfaces  $RA = 0, \pm 0.383$  cut off by the plane  $x = 0$ . The parameters are  $B_{Re} = 1$ ,  $|\kappa|/\eta = 1.83$ ,  $C_3 = -0.548$ .